

STRUCTURE AND PROPERTIES OF As_2S_3 AND As_2Se_3 GLASSES MODIFIED WITH Dy, Sm AND Mn

M. Iovu, S. Shutov, M. Popescu^a, D. Furniss^b, L. Kukkonen^b, A.B. Seddon^b

Centre of Optoelectronics, 1 Academiei Str., MD-2028 Chisinau, Moldova Republic

^aNational Institute of Materials Physics, Bucharest-Magurele, Romania

^bCentre for Glass Research, Department of Engineering Materials,
University of Sheffield, Sheffield, S1 3JD, UK

The effect of low amounts of dysprosium, samarium and manganese (0.1 – 0.5 at.%) on the properties of the chalcogenide glassy semiconductors As_2S_3 and As_2Se_3 is investigated. The metals have significant influence on the structural, optical, electrical and photoelectric characteristics. The fundamental absorption edge shifts towards longer wavelengths with doping. The largest shift was observed for As_2S_3 glasses doped with Dy and Mn. The conductivity is significantly increased by addition of Mn and Dy. All the dopants hamper the photoconductivity with the exception of 0.5 at. % Dy in As_2Se_3 which generates a broad secondary band in the photoconductivity spectrum near 1.05 eV, ascribed to small amounts of crystalline phase. Close correlation was revealed between the medium range order in the network, the metal electronegativity and the activation energy of conductivity.

(Received May 26, 1999; accepted June 9, 1999)

Keywords: Amorphous film, Chalcogenide, Photoconductivity, Arsenic selenide

1. Introduction

Arsenic sulphide As_2S_3 and arsenic selenide As_2Se_3 are typical representatives of chalcogenide glassy semiconductors, with a wide range of applications in optoelectronics, information storage and acousto-optics [1 to 4]. A special interest for those applications is connected with doping of the glasses by active impurities, which alter the electrical and optical properties of the host material. Though it is customary to consider the chalcogenide glasses as insensitive to impurity doping there is ample experimental evidence indicating a significant variation of the glass properties caused by incorporation of small amounts of impurities [5,6].

The aim of this paper is to study the effect of metal impurity on optical, electrical and photoelectrical characteristics of the As_2S_3 and As_2Se_3 glasses doped with Mn, Dy and Sm and to correlate it with the structural details. Manganese is one of the transition metals, which are known to be active as dopants in As_2Se_3 , especially as "modifiers" [7]. Besides, Mn is of interest as it is able to create deep luminescent centers, the optical transitions of which are well understood [8]. As_2S_3 and As_2Se_3 chalcogenide glasses doped with low levels rare-earth elements are thermally stable and are known to be transparent in the mid - IR region (up to 10 - 11 μm). Recently optical fibres of low light losses have been fabricated from Pr^{3+} - doped As_2S_3 glass (0.48 dB/m for $\lambda=1.02 \mu\text{m}$ and 0.17 dB/m for $\lambda=1.3 \mu\text{m}$, respectively) and the effect of light amplification at $\lambda=1.3 \mu\text{m}$ has been demonstrated [9]. For Dy^{3+} - doped As_2S_3 glass the presence of two fluorescence bands due to cascaded transitions ${}^6H_{11/2} \rightarrow {}^6H_{13}$ at 4.40 μm and ${}^6H_{13/2} \rightarrow {}^6H_{15/2}$ at 2.98 μm were detected [10]. It was also shown that As_2S_3 chalcogenide glass fibre is one of the most promising nonlinear optical media for low-power optical switching due to its large refractive index ($n \geq 2.4$) [11], nonlinearity and long interaction length [12]. Besides, some chalcogenide glasses have been used to make IR transmission fibres for imaging, power supply, remote and deformation sensors [13].

2. Experimental

The glasses were synthesized from the elements of 6N (As, S and Se) and 5N (Mn, Sm, and Dy) purity by melting at two temperature steps: at 870-920 K and 1070-1120 K. The concentrations of Mn, Sm and Dy were chosen 0.1 and 0.5 at. %.

The glass transition temperature, T_g , of $As_2S_3:Me$ glasses was measured by the differential thermal analysis (DTA) method. A PERKIN-ELMER equipment 7 Series for Differential Thermal Analysis was used to this purpose (alumina crucible, neutral atmosphere, mass 30 mg, heating rate 10 °C/min, reference calcined alumina). The DTA curves for all glasses are typical for chalcogenide glasses [11]. An increase of T_g from 157 °C for As_2S_3 up to 210 °C for doped glasses was observed.

The structure of the glassy As_2S_3 and As_2Se_3 samples doped by various amounts of metals was investigated by X-ray diffraction procedure. The diffracted intensity curves were measured in a Siemens Kristalloflex IV diffractometer provided with copper target tube and a graphite monochromator mounted in the diffracted beam. A NaI(Tl) water cooled scintillation counter was used in the detection of the diffracted X-ray quanta. Very accurate recordings of the diffraction patterns are necessary due to particular feature of the glass diffractograms (a few broad maxima) and because the expected structural modifications for low metal concentration are quite small. The samples were prepared as powders by crushing chunks of the doped chalcogenide glasses. The powders were pressed in special supports for X-ray diffractometric measurements. High precision diffraction curves have been obtained using the step by step method in the recording of the X-ray intensity. The number of the X-ray quanta was counted for a fixed time (20 s), at every angular position. For different samples an angular increment from $0.005^0(2\Theta)$ to $0.02^0(2\Theta)$ was used.

The characterization of the doped As_2S_3 and As_2Se_3 glasses in the present work was conducted with respect of their specific physical properties. Effect of impurity on arsenic trisulfide, a semi-insulating highly transparent material, was studied by optical methods, while for arsenic triselenide, well known as a photoconductor, the transport properties of doped material were investigated. For optical transmission and absorption measurements bulk polished samples of 2.5 to 3.1 mm thickness were used with an UV/VIS/NIR spectrometer LAMBDA 900 (in the 400-3000 μm spectrum range) and FT-IR spectrometer SPECTRUM 2000 (in the 1.3 to 25.0 μm spectrum range), respectively, PERKIN-ELMER production. Conductivity, spectral distribution and decay of photoconductivity and dependence of the photocurrent upon light intensity were investigated using common techniques for high-resistive samples.

3. Results and discussion

3.1. X-Ray diffraction

After careful investigations of the resulted diffraction curves we have concluded that all the samples are completely amorphous (excepting As_2Se_3 : 0.5 at.% Dy which exhibits a very faint peaks due probably to fine Dy_2Se_3 crystallites) and that the main differences between the curves measured for different glass compositions and various concentrations of modifying elements are related to the angular region comprising the first sharp diffraction peak (FSDP). This means that the doping influences primarily the medium-range ordering in the glassy network.

Fig. 1 and Fig. 2 shows the angular range of the X-ray diffraction curves with the FSDP peak for different metals introduced in the As_2S_3 and As_2Se_3 glassy matrix: Mn, Dy and Sm, with different concentrations. The comparison was made between the samples doped by the minimum metal concentration available (0.1 at.%) and those with the metal concentration of 0.5 at.%. This is important because, during the glass preparation, for every type of doping the preparation of the samples has been carried out in strictly identical conditions. Thus, the eventual fine modifications of the glassy network, as a whole, due to different heating and cooling regime, which can obscure the metal effects, are practically eliminated.

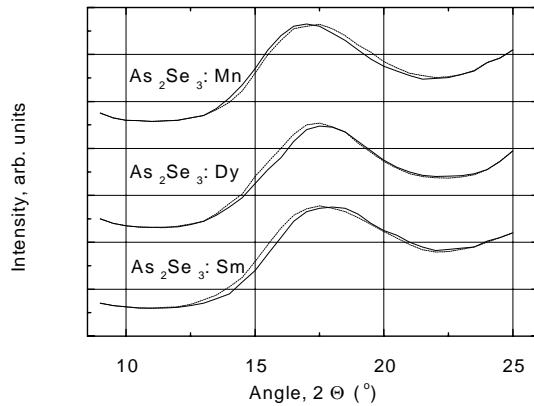


Fig. 1 The X-ray diffraction curves in the region of the first sharp diffraction peak of the metal doped As_2Se_3 glass. -- As_2Se_3 :0.1 at.% Me; — As_2Se_3 :0.5 at.% Me.

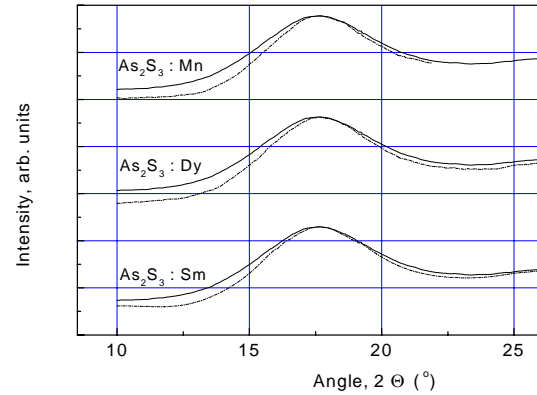


Fig. 2 The X-ray diffraction curves in the region of the first sharp diffraction peak of the metal doped As_2S_3 glass. As_2S_3 (---) and As_2S_3 :0.5 at.% Me(—).

A significant shift of the FSDP from the position corresponding to the pure As_2Se_3 glasses can be observed in the diffraction curves. The direction of the shift depends on the type of the metal introduced in the chalcogenide matrix. We have calculated the per cent of the relative shift of the interlayer distance in the glassy network (as revealed by the position of the FSDP) for every doping metal when the metal concentration in the sample is increased from 0.1 at.% to 0.5 at.%.

Fig. 3 shows the plot of the interlayer distance shift $\Delta d/d(\%)$ versus the per cent of ionicity in the metal-selenium (Me-Se) bond. An interesting linear relation was revealed. This relation convinced us of the importance of the Me-Se interaction for the medium-range order in glass. The As_2Se_3 disordered layers are locally distorted by the insertion of the metal atoms that bonds to selenium. A high covalence of the Me-Se bond gives rise to strong directional bonds and the layers become more rigid while high metal ionicity diminishes the stiffness of the layers. Thus, the intralayer ordering and the interlayer packing are dependent on the type of metal introduced in the As_2Se_3 glass. The samarium (Sm) and dysprosium (Dy) atoms exhibit lower electronegativities (as defined for example by Allred-Rochow) and determine a shift of the interlayer distance towards a lower value [14]. This effect can be ascribed to the role of network modifier of the large rare-earth atoms that smooth the disordered As_2Se_3 layers allowing for a better packing at a smaller thickness. The more ionic Me-Se bonds show lower bond directionality, the layers become more flat and the interlayer distance, corresponding to a better layer packing, decreases [15].

The manganese (Mn), which exhibits higher electronegativity induces a shift of the interlayer distance towards higher values. This effect can be ascribed to the role of network former played by the more covalent atoms. The disordered layers are shifted by the insertion of the atoms with directional bonds. The interlayer distance is increased due to the increase of the effective thickness of the layers. The significant effect of the very low metal concentration in As_2Se_3 chalcogenide glass can be explained by a co-operative effect. The insertion of few dispersed atoms in the layer structure can induce a (dis)ordering at a scale larger than the distance of the first co-ordination spheres and, therefore, the interference between the induced zones can amplify the (dis)ordering [15].

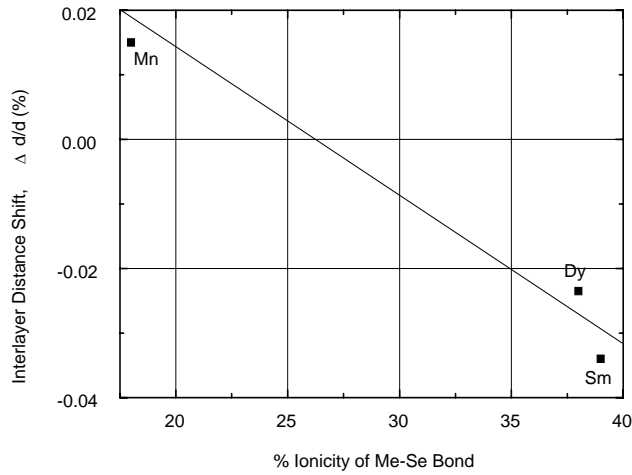


Fig. 3 The relation between the shift of the interlayer distance in As_2Se_3 induced by doping with various metals and the degree of ionicity of the Me-Se bond.

In As_2S_3 , as it is seen from Fig. 2, the above described impurity-induced changes of the glass structure are much weaker, possibly due to larger degree of ionicity of the Me-S bonding in this material.

3.2. Optical absorption

The transmission spectra in the region of absorption edge of $As_2S_3:Me$ chalcogenide glasses are shown in Fig. 4. The addition of heavy rare-earth metals to chalcogenide glass shifts the absorption edge to longer wavelengths and increases the absorbance above the edge. The latter effect is associated with defects generated in the optical gap of a semiconductor by metal atoms. We see that the absorbance in this region increases with growing of Sm concentration from 0.1 to 0.5 at.%. The transmission most strongly falls down in the case of Mn addition: the sample with 0.5 at.% Mn is practically nontransparent in the whole investigated spectral range (0.5 to 25 μm). Strong absorption in a wide spectral interval suggests the alteration of the macrostructure of the material at higher Mn content.

In order to determine the optical gap of the glassy materials under investigation, in Fig. 5 we replotted the edge transmission data in $(\alpha hv)^{1/2}$ vs. (hv) co-ordinates (so called Tauc plot, with α and hv denoting the absorption coefficient and the photon energy, respectively). Except for the Mn-doped sample (curve 4), two nearly straight-line portions are seen in the Tauc plot as is characteristic for many amorphous materials. From the high-energy portion of the plot the values of the optical gap E_g^{opt} were determined; it shifts from 2.2 eV for As_2S_3 to 1.88 eV for the doped glass $As_2S_3:Dy_{0.1}$. Determination of the optical gap for Mn-doped As_2S_3 glasses is not possible.

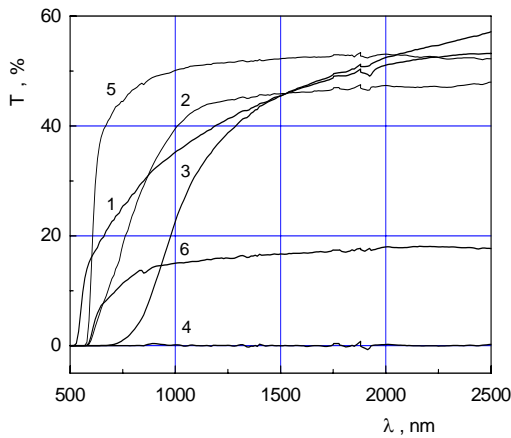


Fig.4 The transmission spectra for or As_2S_3 (1), $\text{As}_2\text{S}_3:\text{Dy}_{0.1}$ (2), $\text{As}_2\text{S}_3:\text{Mn}_{0.1}$ (3), $\text{As}_2\text{S}_3:\text{Mn}_{0.5}$ (4), $\text{As}_2\text{S}_3:\text{Sm}_{0.1}$ (5) $\text{As}_2\text{S}_3:\text{Sm}_{0.5}$ (6).

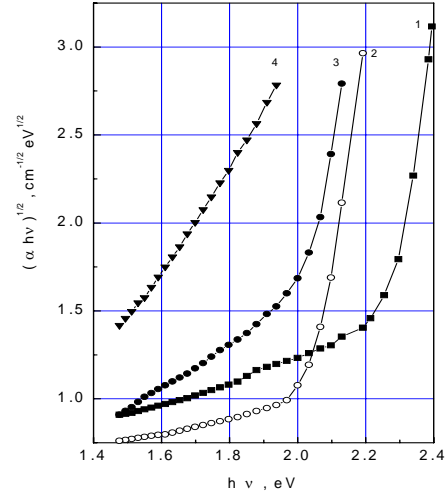


Fig. 5 The absorption spectra for As_2S_3 (1), $\text{As}_2\text{S}_3:\text{Sm}_{0.1}$ (2), $\text{As}_2\text{S}_3:\text{Dy}_{0.1}$ (3), $\text{As}_2\text{S}_3:\text{Mn}$ (4).

The mid-infrared transparency ($1\div 12\ \mu\text{m}$) of the investigated modified chalcogenide glasses is sensitive to impurity as well as to oxygen and hydrogen impurities. Sometimes special technique of preparation and purification of the initial components and glasses are used in order to reduce the absorption bands caused by oxygen, hydrogen and carbon impurities [16,17].

The infrared transmission spectra of $\text{As}_2\text{S}_3:\text{Me}$ glasses are shown in Fig. 6. All As_2S_3 doped glasses are transparent in the near-IR region, with the exception of As_2S_3 doped with 0.5 at.% Mn. All glasses present absorption bands situated at $2.75\ \mu\text{m}$ (H_2O), $4.01\ \mu\text{m}$ (H_2S) and $10.07\ \mu\text{m}$ (As-O-H), which are typical for other chalcogenide glasses [16-19]. The position and intensity of these bands slightly changes in depending on the metal dopant. The absorption bands situated at $7.6\ \mu\text{m}$ and $11.91\ \mu\text{m}$ (As_4O_6) in pure As_2S_3 glass disappear in the doped materials (Table 1). The rare-earth and transition metals are less electronegative than As and might take oxygen from As in the structure.

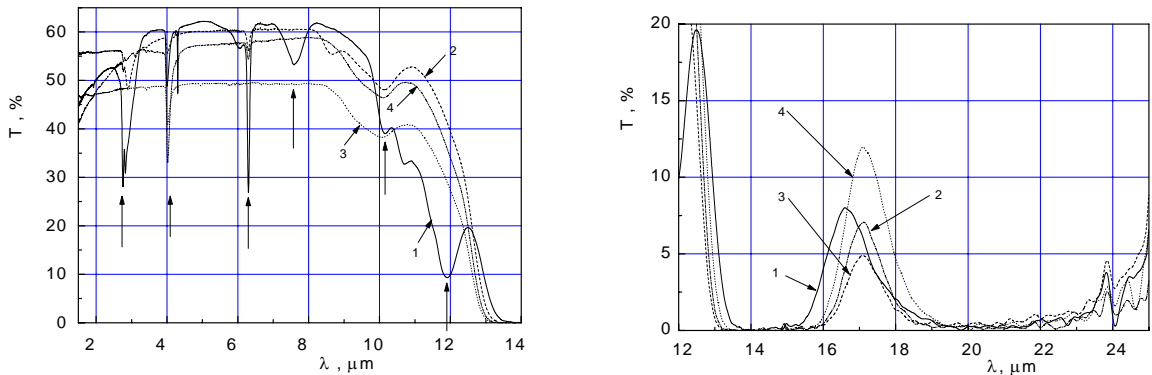


Fig. 6 The transmission spectra for As_2S_3 (1), $\text{As}_2\text{S}_3:\text{Sm}_{0.1}$ (2), $\text{As}_2\text{S}_3:\text{Dy}_{0.1}$ (3) and $\text{As}_2\text{S}_3:\text{Mn}_{0.1}$ (4).

Table 1 Some Absorption Bands for Vitreous As_2S_3 Glass Doped With Dy, Sm and Mn in the Mid-Infrared Region

Glass composition	Band Wavelength (μm) and Possible Species:								
	H_2O	$H_2S - S - H$?	H_2O	?	As_4O_6	As-O in As-O-H	As_4O_6	2- and 3 photon process
As_2S_3	2.75-2.82	3.99-4.03	-	6.29	-	7.58	10.07	11.91	14.22
$As_2S_3:Dy_{0.1}$	-	4.01	-	-	-	-	10.07	-	14.04
$As_2S_3:Sm_{0.1}$	2.76	4.01-4.30	-	6.29	-	-	10.11	-	14.70
$As_2S_3:Sm_{0.5}$	2.76	4.01	4.94	-	6.66	-	10.10	-	14.56
$As_2S_3:Mn_{0.1}$	2.89	4.01	-	6.29	-	-	10.12	-	14.62
$As_2S_3:Mn_{0.5}$	-	-	-	-	-	--	-	--	-

3.3. DC conductivity and photoconductivity

In Table 2 the data of room temperature electrical conductivity σ and activation energy E_0 in the system $As_2Se_3:Me_x$ (Me: Mn, Dy, Sm) are presented. The DC conductivity has been measured in the temperature range: 20-250 °C. Figs. 7 and 8 show the temperature dependence of the conductivity for the bulk samples modified with various metal elements. The dependence of the dark conductivity σ vs. $10^3/T$ for all the glasses $As_2Se_3:Me_x$ glasses could be approximated by a straight line in the range of temperature covered by the measurements. This means that only one activation energy is characteristic for every modified sample. The activation energy, E_0 , is different from one sample to another and depends on the type of metal modifying element. With one exception (0.5 at.% Dy) the E_0 values are higher for the case of the metal modified glasses, when compared to the case of the reference As_2Se_3 sample.

Addition of manganese up to 0.5 at. % increases the conductivity of As_2Se_3 by an order of magnitude, but the activation energy remains approximately unchanged. In the case of the sample with 0.5 at.% Dy, the room temperature conductivity is ten times more than the conductivity of indoped As_2Se_3 , but the activation energy drops to 0.5 eV. The effect upon conductivity of the rising concentration of Dy element can be explained by the presence of a small amount of crystalline phase detected by X-ray diffraction in the sample with 0.5 at.% Dy. Careful measurements of the X-ray diffraction pattern of the sample seems to reveal Dy_2Se_3 very fine crystallites embedded into the rather perfectly amorphous matrix.

At the same time another rare-earth metal dopant, samarium, has little effect on the conductivity of As_2Se_3 , slightly increasing the activation energy and hence decreasing the conductivity at room temperature (Fig. 9 and Fig. 10).

Table 2 Some parameters for the doped As₂Se₃ bulk samples determined from electrical and photoelectrical measurements

Composition As ₂ Se ₃ :Me _x	σ , Ohm ⁻¹ cm ⁻¹	E ₀ , eV	λ_{\max} , μm	$\Delta\lambda_{1/2}$ μm	α
As ₂ Se ₃	1×10^{-12}	0.85	0.821	0.16	0.50
+0.1 at.% Dy	3.49×10^{-13}	0.86	0.821	0.12	0.59
+0.5 at.% Dy	1.17×10^{-10}	0.50	0.821	—	0.61
+0.1 at.% Sm	4.28×10^{-13}	0.94	0.780	0.16	0.70
+0.5 at.% Sm	3.73×10^{-13}	0.94	0.780	0.13	0.57
+0.1 at.% Mn	3.66×10^{-13}	0.97	—	—	0.74
+0.5 at.% Mn	1.08×10^{-11}	0.86	—	—	—

The conductivity data in the case of Mn and Dy suggest the appearance of an additional path of conduction. This path is assumed to be hopping; in the case of Mn these states are deeper than in the case of Dy. From this point of view the increase of the conductivity as well as gradually varying activation energy can be explained.

Doping of As₂Se₃ by the metals under consideration leads to the decrease of the photoconductivity (PC) (i.e. light-to-dark ratio of conductivity), excepting the case of As₂Se₃:0.5 % Dy. Photoconduction is strongly hampered by addition of Mn: 0.1 at. % Mn lowers photocurrent more than two orders of magnitude, and at 0.5 % Mn the photoresponse was not detected. That is why we could not measure the photoconductivity spectra for As₂Se₃:Mn_x. As to dysprosium, with increasing concentration of it from 0.1 at. % to 0.5 at. % the photoconductivity firstly drops down and then increases and exceeds the value for the host As₂Se₃. The spectral parameters for the doped As₂Se₃ samples determined from the photoconductivity spectra (the wavelength at the maximum, λ_{\max} , the halfwidth of the maximum, $\Delta\lambda_{1/2}$) are listed in Table 2.

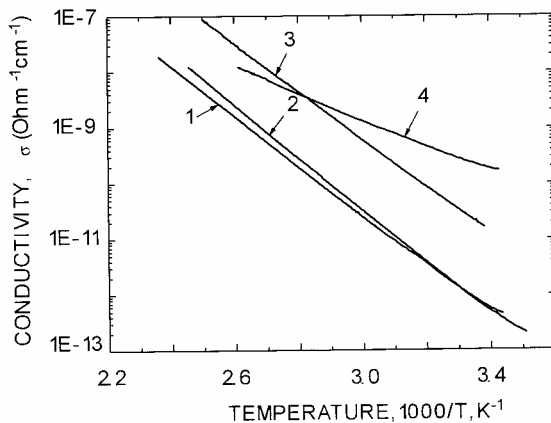


Fig. 7 The temperature dependence of conductivity for As₂Se₃ (1), As₂Se₃:Sm_{0.5} (2) As₂Se₃:Mn_{0.5} (3) and As₂Se₃:Dy_{0.5} (4).

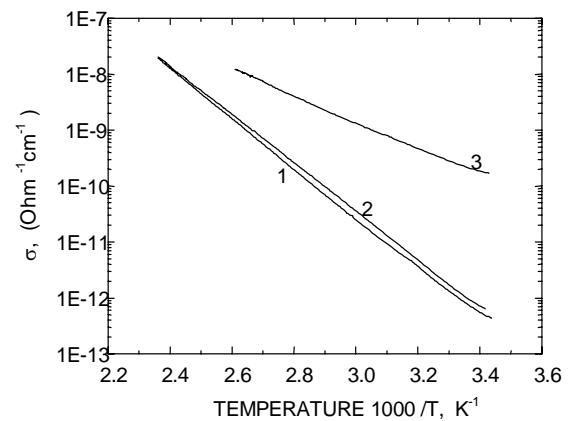


Fig. 8 The temperature dependence of conductivity for As₂Se₃ (1), As₂Se₃:Dy_{0.1} (2) and As₂Se₃:Dy_{0.5} (3).

For all chalcogenide glasses the lux-ampere characteristics of steady-state photoconductivity σ_{ph} in a wide intensity (F) interval are sublinear and exhibit a power law behaviour $\sigma_{\text{ph}}(F) = BF^\alpha$,

where B is a constant weakly dependent on temperature and the power index α is less than unity $0.5 \leq \alpha \leq 1.0$ (Fig. 11 and Table 2). This kind of lux-ampere characteristics may be interpreted by the model of Rose, which assumes an exponential distribution of localized states in the forbidden gap of the amorphous material [20].

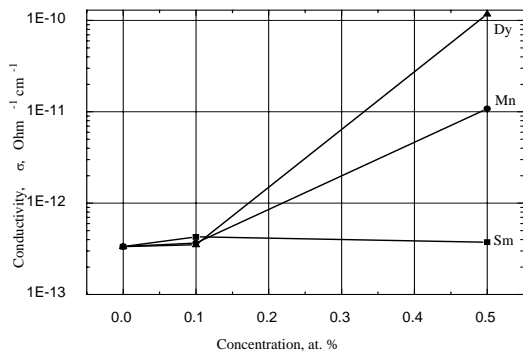


Fig. 9 The dependence of d.c. conductivity σ vs. metal concentration for chalcogenide glasses $As_2Se_3:Me_x$.

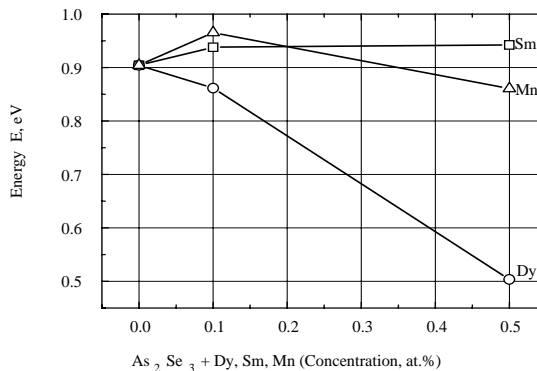


Fig. 10 The dependence of activation energy E_0 vs. metal concentration for chalcogenide glasses $As_2Se_3:Me_x$.

The spectral dependencies of photoconductivity of samples doped with Sm show a single maximum corresponding to the fundamental optical absorption edge. The Sm impurity induces successive shift of the photoconductivity maximum to higher energies from 1.51 eV for As_2Se_3 to 1.59 eV for $As_2Se_3:Sm_{0.5}$. This shift indicates the widening of the optical gap. A similar shift was observed at doping with 0.1 at. % Dy, but at higher Dy concentration (0.5 at. %) a wide band located around 1.05 eV appeared in the photoconductivity spectrum (Fig. 12) [21]. This band can be ascribed to the small amount of crystalline phase revealed in the modified glass.

Finally, it is worthwhile to mention that tin introduced in the As_2Se_3 matrix shifts the fundamental absorption edge towards longer wavelengths (photodarkening effect) as in the case of rare earth doping [22]. For tin modified As-Se films the PD effect is smaller than in non-doped films.

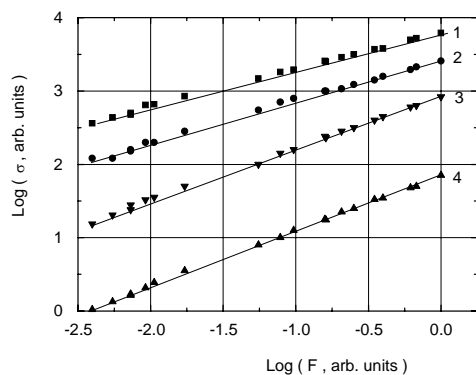


Fig. 11 Photoconductivity vs. light intensity for As_2Se_3 (1), $As_2Se_3:Dy_{0.1}$ (2), $As_2Se_3:Sm_{0.1}$ (3) and $As_2Se_3:Mn_{0.1}$ (4).

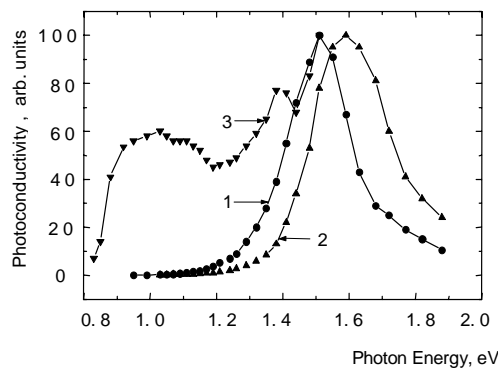


Fig. 12 The spectral dependence of photoconductivity for As_2Se_3 (1), $As_2Se_3:Sm_{0.5}$ (2) and $As_2Se_3:Dy_{0.5}$ (3) glasses.

4. Conclusions

There was shown, that doping of the As₂S₃ and As₂Se₃ glasses by small amounts of metals (in this paper a transition metal, manganese, and two lanthanides, samarium and dysprosium), determines measurable optical and electrical effects. The electrical conductivity is influenced by metals both in the dark and, especially, under photoexcitation. The doping atoms induce the shift of the absorption edge of As₂S₃ glass to the low energy region and increase the absorption in the sub-band region. In the mid-IR region an effect of removing the absorption bands associated, probably, with arsenic oxides was observed in doped samples. Deep localized states are created in the energy gap of the modified As₂Se₃ glass, with rather high density, which is clearly manifested as a band in the photoexcitation spectra (0.5 at. % Dy) or as additional paths of conduction (0.5 at. % Mn and 0.5 at. % Dy). In the case of As₂Se₃ film modified by 0.5 at.% Dy this feature can be partially related to a small amount of a crystalline phase with very low crystallite size. The deep impurity centers increase the recombination rate leading to strong quenching of the photoconductivity in most considered cases of metal addition. The X-ray diffraction results indicate a significant modification of the mean distance between the disordered layers, induced by metals.

Acknowledgement

This work was partially supported by the Royal Society Exchange Programme. One of us (M.I.) is grateful for the possibility offered to carry out research in the Centre of Glass Research (University of Sheffield) in the Department of Material Engineering lead by Dr. A.B. Seddon.

References

- [1] Madan A., Shaw M.P., *The Physics and Application of Amorphous Semiconductors*, Academic Press, 1988.
- [2] Popescu M., Andriesh A., Chumash V., Iovu M., Shutov S., Tsiuleanu D., *The Physics of Chalcogenide Glasses*, Ed.Stiintifica Bucharest - Ed.Stiinta Chisinau, 1996.
- [3] Seddon A.B., in "Physics and Applications of Non-Crystalline Semiconductors in Optoelectronics", Ed, by A.Andriesh and M.Bertolotti, Kluwer Academic Publishers, NATO Series. 3. High Technology, v. 36, pag. 327, 1977.
- [4] Andriesh A.M., *Sov. Semiconductors* **32**, 867(1998).
- [5] Trnovcova V., *Czechoslovak J. of Physics* **A30**, 345(1980).
- [6] Elliot S.R., *Adv. Phys.* **36**, 135(1987).
- [7] Kolomiets B.T., Averyanov V.L., in "Physics of Disordered Materials", New-York, London, pag. 663, 1985.
- [8] Grimmeiss M.G., Ovren C., Allen J.W., *J. Appl. Phys.* **47**, 1103(1976).
- [9] Ohishi Y., Mori A., Kanamori T., Fujiura K., Sudo S., *Appl. Phys. Lett.* **65**, 13(1994).
- [10] Heo J., *J. Mat. Sci. Lett.* **14**, 1014(1995).
- [11] *Properties, processing and application of Glass and Rare Earth-Doped Glasses for Optical Fibers*, ed. By D.Hevak, INSPEC, London, 1998.
- [12] Asobe M., Ohara T., Yokohama I., Kaino T., *Electronics Letters* **32**, 1396; 1611(1996).
- [13] Andriesh A., Abashkin V., Binchevichi V., Culeac I., Necshoiu T., Aftimei A., Miclosh S., Zisu T., *-Romanian Reports in Physics* **47**, 239(1995).
- [14] Andriesh A., Iovu M., Popescu M., Sava F., Lorinczi A., Shutov S., *Balkan Phys. Letters* **5**, 146(1997).
- [15] Iovu M., Shutov S., Bulgaru M., Popescu M., *Proceed. Intern. Semicond. Conf., CAS'96, Sinaia, Romania*, pag. 313, 1996.
- [16] Churbanov M.F., *J. Non-Cryst. Solids* **184**, 25(1993).
- [17] King W.A., Clave A.G., LaCourse W.C., *J. Non-Cryst. Solids* **181**, 231(1995).
- [18] Zhenhna L., Frischat G. H., *J. Non-Cryst. Solids* **163**, 169(1993).
- [19] Seddon A.B., *J. Non-Cryst. Solids* **184**, 44(1993).

- [20] Rose A., Concepts in Photoconductivity, Moscow, Mir Publishing House, 1966.
- [21] Iovu M., Bulgaru M., Shutov S., Balkan Phys. Letters **4**,147(1996).
- [22] Iovu M., Shutov, S., J. Optoelect. and Adv. Mat. **1**, 1(1999).